



EXPERIMENTAL STUDY OF FORMATION OF DETONATION WAVE DRIVEN BY CONDENSATION OF SUPERSATURATED CARBON VAPOR

Alexander Emelianov¹, Alexander Eremin², Vladimir Fortov², Alexander Makeich², Helga Jander³,
Joachim Deppe⁴

ABSTRACT

In the work experimental observation the formation of detonation wave initiated by the energy release of condensation of supersaturated carbon vapor are presented. One of the most important results of these observations is the fact that the process of condensation of supersaturated carbon vapor can occur in explosive mode and the released energy can be transmitted very efficiently to the formation of detonation waves. The experiments were conducted behind reflected shock waves in the mixtures initially containing 10–30% C_3O_2 in Ar. Initial temperatures and pressure behind the reflected wave (before chemical transformations) were varied in the range 1300-1800K and 4-9 bar. Analysis of obtained results has shown that in the mixture 10% C_3O_2 +Ar the insufficient heat release resulted in overdriven detonation due to remaining support of the wave propagation by the pressure behind it. In the mixture 20% C_3O_2 +Ar a very good coincidence of measured values of pressure and wave velocity with the Chapman-Jouguet parameters of detonation, calculated using a one-dimensional approximation is observed. In more rich mixture 30% C_3O_2 +Ar the measured values of pressure and wave velocity lie below the calculated parameters of detonation.

Keywords: shock wave, condensation, detonation, supersaturated carbon vapor

INTRODUCTION

The great numbers of works are devoted to study of condensed particles formation at combustion and detonation of gaseous hydrocarbon fuels (Oppenheim 2008). Condensation process as well as oxidation reaction are characterized by an essential heat release and possibility of use of this energy for creation of a detonation wave is quite probable. In the work (Vasil'ev & Pinaev 2008) process of formation carbon nanoparticles behind detonation waves in acetylene-air and acetylene-oxygen mixtures has been investigated, however the quantitative contribution of energy of condensation is not discussed in detail. In the given work results of experimental observation of formation of a detonation wave at condensation of supersaturated carbon vapor are presented.

In the recent experiments (Emelianov *et al.* 2007), the considerable heating of reacting mixture, caused by the condensation of carbon vapor formed during the shock wave pyrolysis of carbon suboxide C_3O_2 , has been observed. Carbon suboxide is a rather unstable volatile compound and under

¹ Corresponding author: Joint Institute for High Temperatures, Russian Academy of Sciences, e-mail: aemelia@ihed.ras.ru

² Joint Institute for High Temperatures, Russian Academy of Sciences

³ Institut für Physikalische Chemie, Göttingen Universität, Germany

⁴ LaVision, Göttingen, Germany

heating up to 1400 – 1600 K its molecules decompose to carbon atom and two CO molecules. Experiments (Emelianov *et al.* 2007) have shown that complete transformation $C_3O_2 \rightarrow CO + \text{carbon nanoparticles}$ in the mixtures containing only 3% C_3O_2 in Ar resulted in the temperature rise up to 300 K. An important peculiarity of this process is that a bottleneck of condensed particle growth is the reaction of carbon vapor formation, exponentially accelerating with the temperature (Doerge *et al.* 1999). At the temperatures 1800 – 2500 K and pressures 3 – 30 bar a stage of cluster growth up to the sizes $10^3 - 10^4$ atoms, which is accompanied by the active heat release, lasts at about 1 – 10 μs (Emelianov *et al.* 2005). Therefore at appropriate conditions the process of energy liberation can proceed in a heat explosion regime and form a self-sustaining detonation wave (Emelianov *et al.* 2009). Another important property of the process of C_3O_2 decomposition and consequent carbon condensation is the total absence of secondary gaseous reactions (in the system remains only CO, which is chemically stable at $T < 4000\text{K}$). This fact presents the opportunity to perform a reliable analysis of interconnection of cluster growth and heat release behind shock waves of various intensities. The goal of this work was the visualization and detailed experimental study of the formation of detonation wave of condensation.

EXPERIMENTS

Experiments were performed behind reflected shock waves in a diaphragm-type shock tube with an inner diameter of 70 mm, a 2.5-m long driver section and a 4.5-m long driven section. The propagation of reflected shock wave in the mixtures initially containing 10–30% C_3O_2 in Ar has been studied. The carbon precursor - C_3O_2 was produced in an independent apparatus by dehydration of malonic acid, bis (trimethylsilyl) ester with phosphor pentoxide at a 165°C. Its purity was checked by vapor pressure measurements and by FTIR spectroscopy.

The pressure and temperature behind incident shocks were 0.8–1 bar and 800–1100 K, respectively. Chemical reactions involving C_3O_2 were negligible for such parameters (Doerge *et al.* 1999). The calculated “frozen” (before chemical transformations) temperature and pressure behind the reflected shock ranged from 1490 to 1750 K, and 4 – 9 bar correspondingly. The actual pressure and shock wave velocity were measured by several piezo-gauges installed at the various distances 0 – 300 mm from the end plate of shock tube. For the observation of shock wave behavior the shock tube was equipped by two rectangular sapphire windows 160 mm x 5 mm installed on the distance 25 mm from the end plate (see Fig.1). Through these windows the time resolved images of radiation behind shock wave in the range 300 – 800 nm were recorded using an ICCD camera (StreakStar II, LaVision GmbH). Besides that the laser light attenuation (or extinction) at $\lambda = 633 \pm 10$ nm, depicting the condensed particle formation, was registered through the same windows at the different distances from the end plate. In Fig. 1 the scheme of experimental setup and the main methods of diagnostics are presented.

In Fig.2 the schematic of the measuring section of shock tube and example of the records of ICCD camera and pressure gauges in the test experiment in the mixture 1% $C_6H_6 + \text{Ar}$ at the temperature $T_5 = 2800$ K are shown. At these conditions particles are formed during $\sim 10 \mu\text{s}$ without any essential heat effects (Drakon *et al.* 2007).

In the next Fig.3 several examples of experimental records of pressure, emission and extinction, measured in the mixtures $C_3O_2 + \text{Ar}$ are demonstrated. Fig. 3A shows the propagation of shock wave in the mixture 10% $C_3O_2 + 90\% \text{Ar}$, when the “frozen” temperature behind the wave is $T_5 = 1390\text{K}$.

At this relatively low temperature the chemical transformations of C_3O_2 during the residence time are negligible (Doerge *et al.* 1999) and shock wave demonstrates a steady velocity ($V_5 = 920$ m/s) and pressure, no radiation and no extinction, excepting the sharp schlieren signal at the moment of shock front propagation. Fig. 3B represents experimental plots, observed in the same mixture 10% $C_3O_2 + 90\% \text{Ar}$, when the calculated velocity of reflected shock wave was $V_5 = 1040$ m/s and “frozen” temperature was higher - $T_5 = 1620\text{K}$. At this temperature the process of C_3O_2 decomposition and carbon particle formation proceeds quite effectively and one can see that immediately after

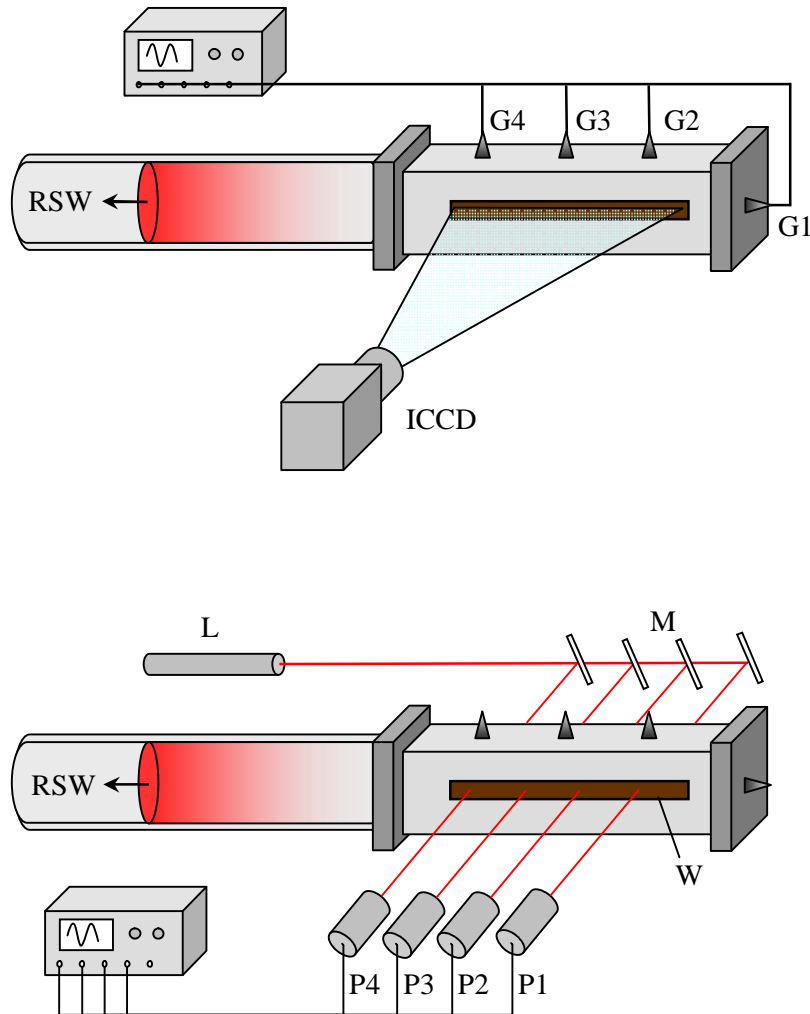


Fig. 1. Scheme of a shock tube and multichannel diagnostics of formation of a detonation by means of pressure gauges (G1-G4), laser extinction and radiation of a flow by means of photomultiplier (P1-P4), and time development of radiation with the use Streak-Star camera LaVision (ICCD). L – the laser, M – system of mirrors, W – a sapphire window, RSW – the reflected shock wave.

achievement of calculated values of pressure behind a shock wave front $P_5 = 4.5$ bar (dashed line) an additional pressure rise up to about 6 bar is observed. Further propagation of shock wave is characterized by the noticeable increase of its velocity up to $V_{exp} = 1290$ m/s and appearance of sharp pressure peak just behind the front. These processes are accompanied by the rise of radiation peaks testifying to essential temperature increase in the narrow zone behind the wave front. Lower row of records demonstrates a rise of extinction, reflecting the formation of condensed particles. Obviously that the condensation process is also accelerating with the propagation of the wave. In the mixtures containing 20% C_3O_2 (Fig 3C) much faster and more intensive acceleration of the shock wave from $V_5 = 1090$ m/s up to $V_{exp} = 1490$ m/s, accompanied by the formation of sharp peaks of pressure and radiation as well as step-wise condensation has been observed. The profiles of pressure and radiation, shown in Fig. 3C, are quite typical for gaseous detonation waves (Zverev & Smirnov 1987).

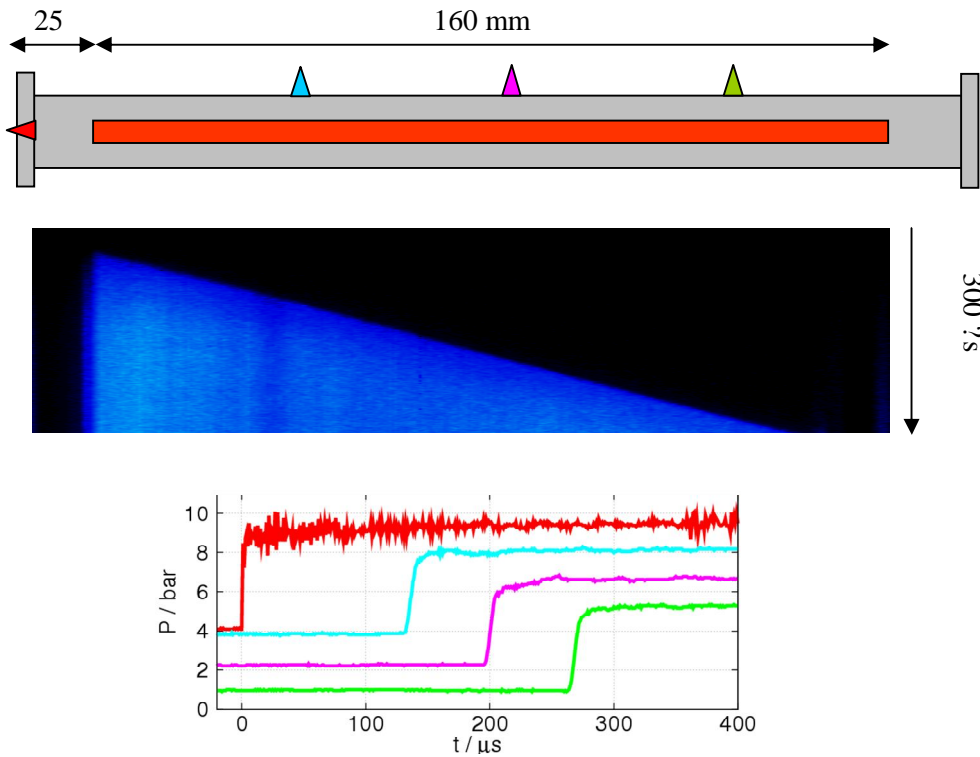


Fig. 2. Schematic of the section of shock tube with the measurement windows, example of time and distance resolved record of radiation intensity behind reflected shock wave, measured by ICCD camera, and the time profiles of pressure, registered by piezo-gauges in the testing experiment in the mixture 1% C_6H_6 + Ar at the temperature $T_5 = 2800$ K.

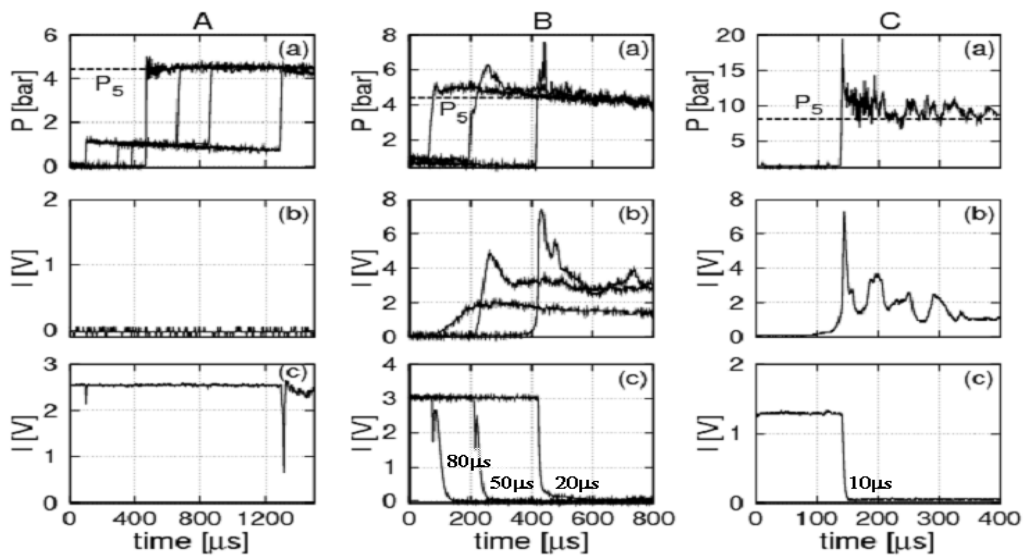


Fig.3. The time profiles of pressure (a), radiation at 633 nm (b) and laser light extinction (c), measured behind shock waves in the mixtures C_3O_2+Ar at various distances (70 mm, 140 mm and 295 mm) from the end plate of shock tube. Mixtures and “frozen” temperatures T_5 behind the wave near end plate are: A – 10% C_3O_2+Ar , $T_5 = 1390K$; B - 10% C_3O_2+Ar , $T_5 = 1620K$; C - 20% C_3O_2+Ar , $T_5 = 1440K$. Digits in the plots B(c) and C(c) show the characteristic time of extinction rise.

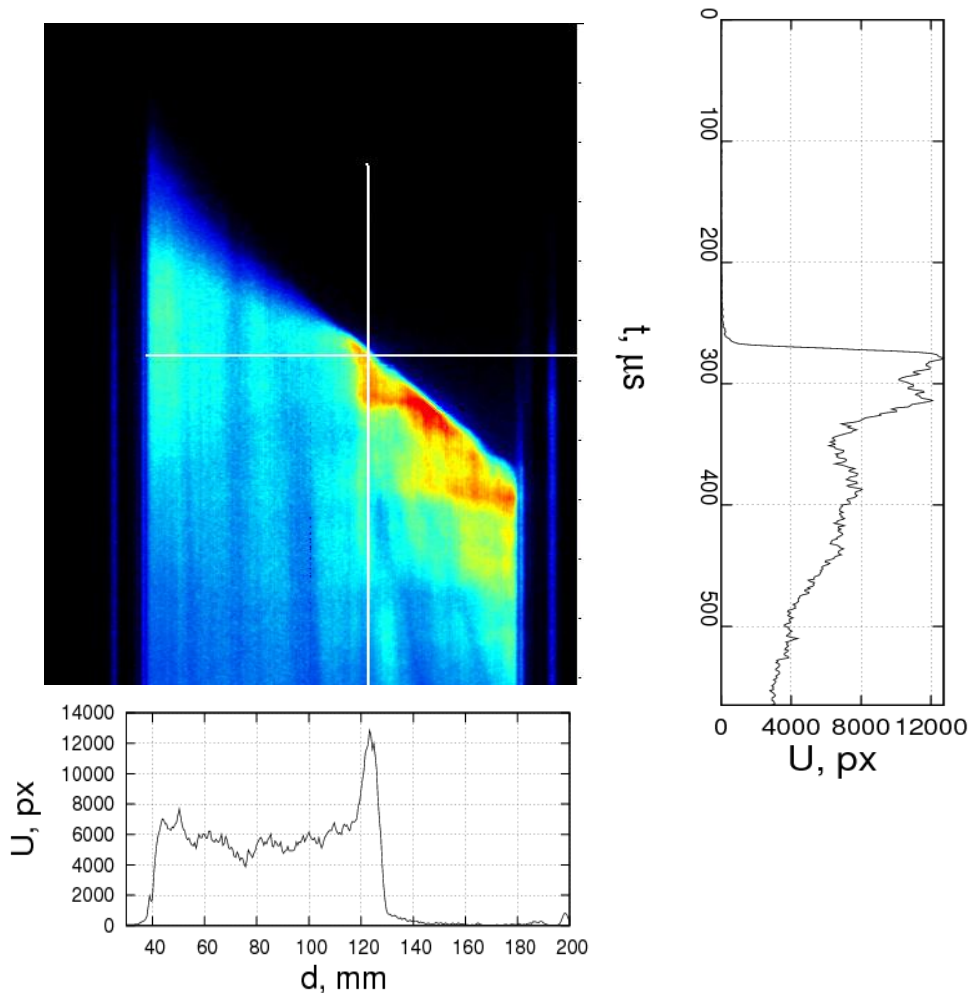


Fig.4. The time-scanning images of radiation measured by ICCD camera and selected vertical and horizontal radiation profiles in mixture 10% $\text{C}_3\text{O}_2 + \text{Ar}$. $T_5(\text{frozen})=1650\text{K}$, $V_5(\text{frozen})=1100\text{m/s}$.

In Fig.4-6 the pictures of time-scanning of radiation behind the shock waves recorded by ICCD camera and selected vertical and horizontal profile versus time and distance correspondingly in the mixtures, initially containing different amount C_3O_2 in Ar, are shown. The “frozen” temperatures T_5 in all cases are so low that radiation of the mixture before the heat release processes could not be seen. However after conjunction of condensation and the shock wave a bright radiation appears with the typical peaks near the front clearly seen on all selected profiles.

In the first case of 10% C_3O_2 (Fig.4) the heat release condensation wave overtakes the shock wave front somewhere at the middle of the window and speeds it up to the 1300 m/s against the initial value $V_5 = 1100\text{m/s}$. In the mixture 20% C_3O_2 (Fig.5), despite of the less “frozen” temperature, the condensation wave overtakes shock front much earlier and supports the stable shock wave velocity ~ 1500 m/s (against initial $V_5 = 1050\text{m/s}$). And in the mixture 30% C_3O_2 (Fig.6) shock front first accelerates from $V_5 = 1100$ m/s up to 1600 m/s and then slows down to 1300 m/s. Obviously that these pictures qualitatively are in accordance with the records of the radiation measured by photomultipliers (see Fig. 3(b)).

In the first picture Fig.4 the brightest picture of development of detonation-like structure behind shock wave front measured in the mixture 10% $\text{C}_3\text{O}_2 + \text{Ar}$ is clearly seen. In the next Fig.7 several snap-shots of radiation intensity, extracted from this picture, are presented. The position of shock wave front, marked by the red line, was determined from the pressure gauges measurements. One can see that radiation begins to grow near the end plate of shock tube, when shock wave front is already at

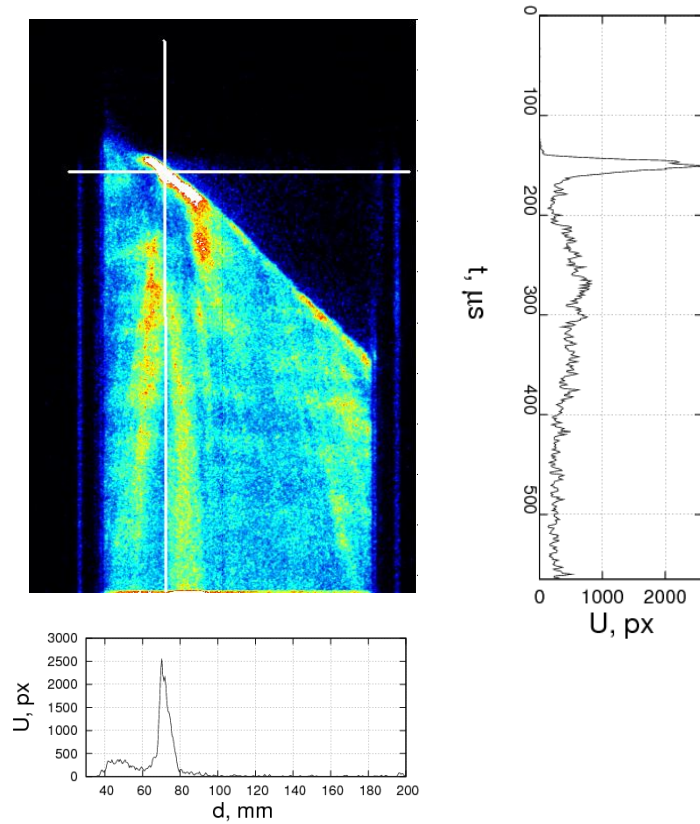


Fig.5. The time-scanning images of radiation measured by ICCD camera and selected vertical and horizontal radiation profiles in mixture 20% $\text{C}_3\text{O}_2 + \text{Ar}$. $T_5(\text{frozen})=1530\text{K}$, $V_5(\text{frozen})=1050\text{m/s}$.

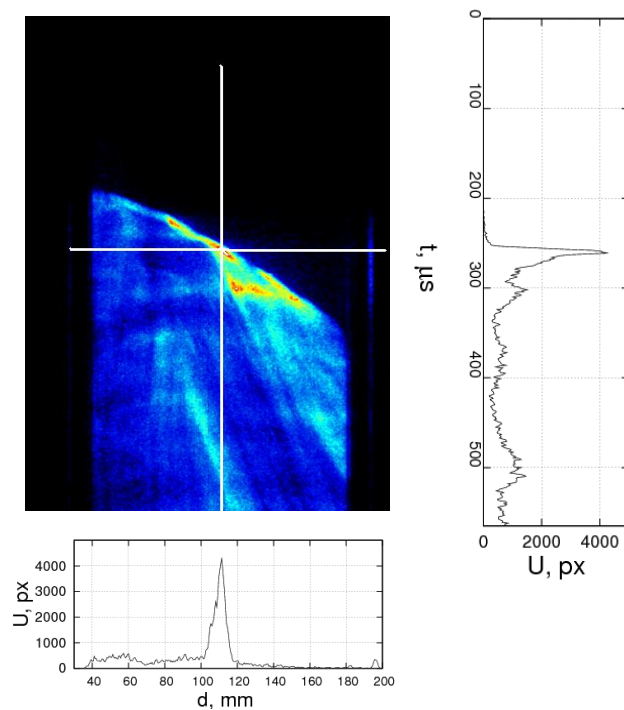


Fig.6. The time-scanning images of radiation measured by ICCD camera and selected vertical and horizontal radiation profiles in mixture 30% $\text{C}_3\text{O}_2 + \text{Ar}$. $T_5(\text{frozen})=1490\text{K}$, $V_5(\text{frozen})=1100\text{m/s}$.

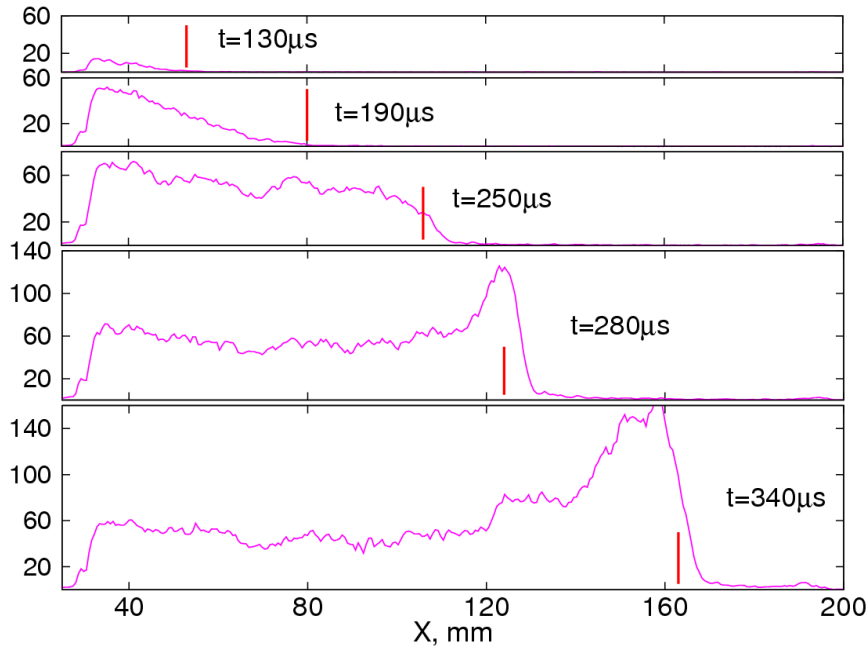


Fig.7. Several snap-shots of radiation intensity, extracted from the data, measured by ICCD camera, shown on the picture of Fig.4.

55 mm away from the end. Then radiation increases and gradually comes up to the front. Finally, at the distances more 120 mm from the end plate the radiation overtakes the front and typical detonation-like structure of radiation intensity is formed. Looking on the traces, shown in Fig.3. B, which have been measured in the very similar conditions, it is clear that sharp rise of radiation is completely caused by the fast heat release of the immediate condensation behind the shock wave front.

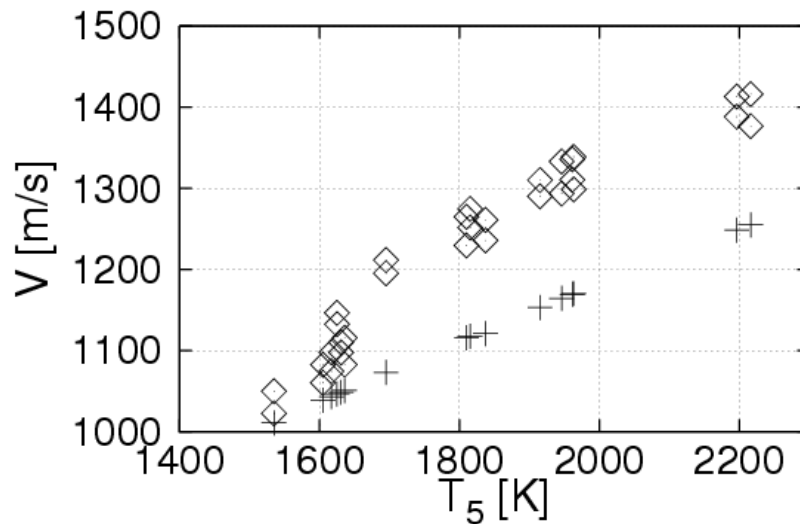


Fig.8. Comparison of shock wave velocity V_{exp} (\diamond) measured at 195 mm from the tube end with the values V_5 (+) calculated for “frozen” conditions for 10% C_3O_2 +Ar.

In Fig.8 the temperature dependence of shock wave velocity measured in the mixture 10% C_3O_2 +Ar at 195 mm from the end plate of the shock tube is compared with the computed values for “frozen” conditions. The acceleration of the shock wave starts at the temperatures above 1500 K, corresponding to onset of the thermal decomposition of C_3O_2 (Doerge *et al.* 1999). At temperatures above 2500 K the velocity difference comes to a maximum indicating the entire input of the

condensation energy to the dynamic of the shock wave. Note that the control experiments in non-reacting mixtures showed a very good agreement between the calculated and measured velocities of the reflected shock wave ($\Delta V/V \leq 0.01$).

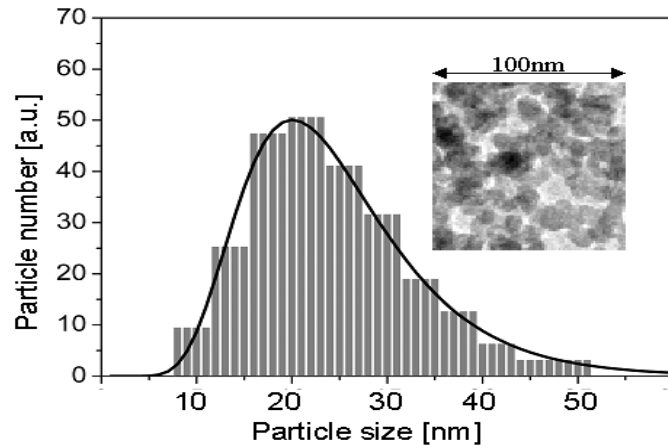


Fig.9. Size distribution of carbon nanoparticles formed behind the shock wave in the mixture 20% C_3O_2 +Ar.

DISCUSSION

To analyze the observed phenomena, recent data on the heat release of carbon particle formation during the thermal decomposition of C_3O_2 behind shock waves (Emelianov *et al.* 2007) were used.

Numerical calculations of the kinetics of C_3O_2 dissociation and the subsequent condensation of carbon vapor, accounting for the energy balance of each reaction, were performed using the kinetic scheme proposed in (Wagner *et al.* 2001). The total heat, Q , released from the reaction:



is calculated from

$$Q = \Delta H_f(C_3O_2) - 2\Delta H_f(CO) - \Delta H_f(C_N)/N$$

where ΔH_f are the enthalpies of formation of the mixture components. In the above reaction, N is the number of carbon atoms in a particle.

The main uncertainty in the calculations was caused by the lack of reliable data on the equations of state and enthalpies of formation of carbon nanoparticles of various sizes. In Fig.10 the approximation $Q = f(N)$, based on data taken from Refs. (Emelianov *et al.* 2007), (Chase *et al.* 1985) and (Martin *et al.* 1991), is presented. According to the accepted values, the dissociation energy of C_3O_2 (~573 kJ/mol) is already compensated for at the cluster size $N \approx 20$ atoms, and later the process becomes exothermic.

Condensed carbon nanoparticles formed behind the wave were collected after experiments and analyzed using X-ray spectroscopy and electron microscopy. Particles consist of pure carbon, have a structure of amorphous graphite and look like a spheres with an average size ~ 15 – 30 nm (see Fig.9).

One can see from Fig.10 that at final particle size 20 nm (that corresponds at particle density 1.86 g/cm³ (Kirk & Othmer 1992) to $N \approx 10^6$ atoms) the heat of reaction approaches ~ 100 – 120 kJ/mol.

An efficiency of contribution of condensation energy to the shock wave dynamic strongly depends on the real time of particle growth up to the final size. Qualitatively this time can be estimated from the extinction profiles shown in Fig.3(B,C). One can see that with the amplification of shock wave (and the corresponding temperature rise) this time decreases from 80 to 10 μ s. It was already

mentioned above that the reason of apparent acceleration of condensation with the temperature rise is that the rate determining step of the whole process is the reaction of decomposition $C_3O_2 \rightarrow CO + C_2O$ which has the rate constant $k_d = 2 \cdot 10^{15} \exp(-225 \text{ kJ/mol/RT}) \text{ cm}^3 \text{ mol}^{-1} \text{ s}^{-1}$ (Doerge *et al.* 1999), all other reactions proceed faster. In experiments (Emelianov *et al.* 2007) it was shown that up to the temperatures $T \geq 2200 \text{ K}$ the effective rate constant of particle growth practically coincides with k_d . However such a behavior of the process is correct until the reversal reactions of nanoparticle decay come into play. Toward higher temperatures particle formation rate becomes slower (Deppe *et al.* 2000). At $T = 3000 \text{ K}$ the total particle rise time is more than $100 \mu\text{s}$ and at $T = 3400 \text{ K}$ the rate of particle decay (evaporation) is already higher than the formation rate. Therefore it is obviously that, in contrast to classical detonation caused by the combustion processes, given phenomenon must have an extreme on integral heat release and at excessive overheating the process shall become self-destructive.

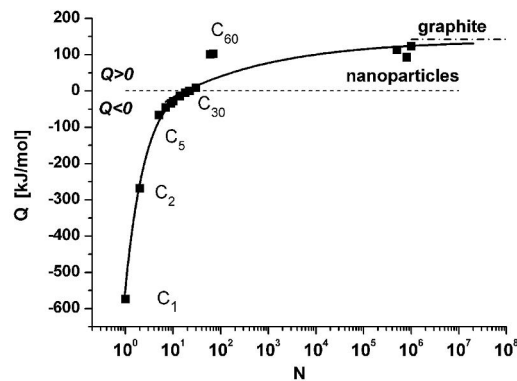


Fig. 10. Total heat balance of the process $C_3O_2 \rightarrow 2CO + (1/N)CN$ as a function of the final particle size N .

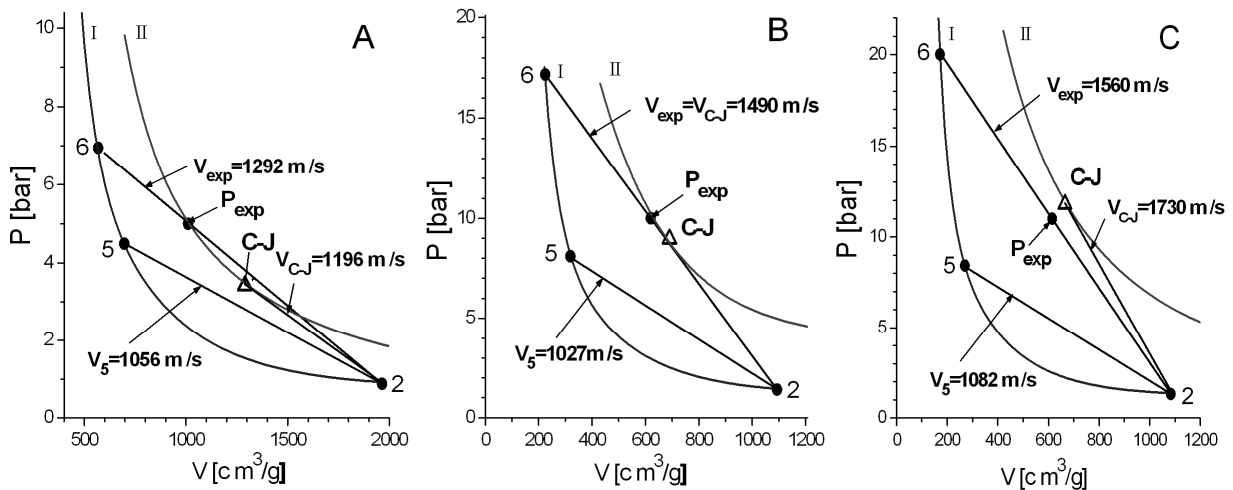


Fig. 11. The behavior of Hugoniot adiabatic curves for the initial mixtures (curves I) and for the mixtures after condensation (curves II). A - mixture 10% $C_3O_2 + Ar$, $T_{C-J} = 2050 \text{ K}$; B - mixture 20% $C_3O_2 + Ar$, $T_{C-J} = 2460 \text{ K}$; C - mixture 30% $C_3O_2 + Ar$, $T_{C-J} = 2830 \text{ K}$.

These reasoning are clearly illustrated in Fig.11 (A,B,C) by the comparison of observed shock wave parameters with the behavior of Hugoniot adiabatic curves for the initial mixtures (curves I) and for the mixtures after condensation (curves II). Straight lines 2 – 5 correspond to calculated velocity of reflected shock wave. Points 6 and rays 2 – 6 represent the experimentally measured pressure maxima and velocity of accelerated wave front. Points P_{exp} on the rays 2 – 6 show the steady pressure values and the points C-J on the curves II demonstrate the Chapman-Jouguet parameters of detonation,

calculated in 1D approximation (Zverev & Smirnov 1987). One can see that in the mixture 10% C_3O_2+Ar ray 2 – 6 intersects adiabat 2 at the pressures, which are consistent with the values measured in experiments - P_{exp} and noticeably higher than P_{C-J} . Besides that a velocity of the wave is a bit higher than Chapman-Jouguet velocity (tangent to curve II from point 2). This behavior of the wave is likely caused by the insufficient heat release resulting in remaining support of the wave by pressure behind it. Such a flow regime is usually called “overdriven detonation”.

In the mixture 20% C_3O_2+Ar a good coincidence of measured and calculated values of pressure and wave velocity is observed. At these conditions the calculated temperature behind the detonation front is 2460 K that according to (Deppe *et al.* 2000) corresponds to maximum condensation rate. This fact is clearly demonstrated by the extinction profile in Fig.2C.

In richer mixture 30% C_3O_2+Ar the measured values of pressure and wave velocity lie below the calculated parameters of detonation. This fact could be explained by the excess heat release resulting at incomplete condensation at the temperature rise above 2800 K. At these temperatures the reversal processes of particles decay, slowing down the effective condensation rate, begin to play a role. Due to that the energy of condensation can not be completely transmitted to the wave dynamic and so-called regime of “underdriven”, damping detonation is observed.

CONCLUSION

In this paper the complex of experimental techniques, including the Streak-camera, multi-channel emission, extinction and pressure measurements was applied for the investigation of a principally new phenomenon – the formation of a detonation wave of condensation. The obtained data clearly demonstrate the process of shock wave acceleration and formation of typical structure of detonation wave, initiated by the explosive condensation of supersaturated carbon vapor.

ACKNOWLEDGEMENT

The support of this work by Russian Academy of Sciences and RFBR is gratefully acknowledged.

REFERENCES

- Oppenheim A. K. (2008) Dynamics of Combustion Systems, Springer, Berlin, pp. 299–343.
- Vasil'ev A. A., Pinaev A. V. (2008) Formation of carbon clusters in deflagration and detonation waves in gas mixtures. Combustion, Explosion, and Shock Waves. 44: 317.
- Emelianov A.V, Eremin A.V, Makeich A.A, et al. (2007) Heat release of carbon particle formation from hydrogen-free precursors behind shock waves. Proc. Comb. Inst. 31: 649.
- Doerge K.J, Tanke D, Wagner H.Gg. (1999) Particle formation in carbon suboxide pyrolysis behind shock waves. Z. Phys.Chem. 212: 219.
- Emelianov A.V, Eremin A.V, Gurentsov E.V, Makeich A.A., Jander H.K., Wagner H. Gg. (2005) Time and temperature dependence of carbon particle growth in various shock wave pyrolysis processes. Proc. Comb. Inst. 30: 1433.
- Emelianov A., Eremin A., Fortov V., Jander H., Makeich A., Wagner H.Gg. (2009) Detonation Wave Driven by Condensation of Supersaturated Vapor. Physical Review E, **79** (3), 035303-(1-4).
- Drakon A.V., Emelianov A.V., Eremin A. V., Makeich A. A., Schulz C. (2007) Phys-Chem. Kin. in Gasdynamics. 5, www.chemphys.edu.ru/pdf/2007-09-17-001.
- Zverev I. N., Smirnov N. N. (1987) Gas Dynamics of Combustion, MGU, Moscow, p. 307.
- Wagner H. Gg., Vlasov P. A., Doerge K. J., et al. (2001) Kinetika Kataliz. 5, 645.
- Chase M. W. Jr., Davies C. A., Downey J. R., Frurip Jr., D. J., McDonald R. A., Syverud A. N. (1985) *JANAF Thermochemical Tables*, 3rd ed., Parts I - II, J. Phys. Chem. Ref. Data 14, Suppl. 1.
- Martin J. M. L., Francois J. P., Gijbels R. (1991) J. Chem. Phys. 95, 9420.
- Kirk A. F., Othmer D. F. (1992) Encyclopedia of Chemical Technology. V.4 (John Wiley and Sons, 4th Edition), p. 1039.
- Deppe J., Emelianov A., Eremin A., Jander H., Wagner H. Gg., Zaslanko I. (2000) Proc. Combust. Inst. 28, 2515.